Reliability Assessment of Power System based on Load Flow Analysis of the IEEE 57 Bus used in Micro Grid Applications

G. VEERA BHADRA CHARY[1], RAGHAVAIAH KATURI[2*], K. MERCY ROSALINA[3]
Department of Electrical and Electronics Engineering,
VFSTR deemed to be University, Vadlamudi,
Guntur, Andhra Pradesh,
INDIA

Corresponding Author

Abstract: - The complex power system consists of more interconnections; therefore, modelling such a type of network is a very difficult task in the commercialization area cycle. MATPOWER has all steady-state power system models, which are extensively used in academic research for power flow (PF) modeling. The PF architecture designed in this is extensible; it is easy to add or modify variables and constraints in the standard case structure. This paper presents the details of the mathematically scaled loads in IEEE 57 bus power system network modelling by using the standard test case data. Internally, all the bus voltages are expressed in p.u., and phase angles are expressed in radians, but the generators and loads are expressed in terms of power ratings. The scaling of these is defined based on the scaled voltage of the corresponding bus voltage. The scaling load procedure used in this paper is very useful for designing a low-voltage power system network for practical analysis purposes. Two simulations are performed in this paper for the analysis of the actual load flow (ALF) and scaled load flow (SLF) power system models. The voltage, phase angle, and power flow through the lines are compared to analyze the accuracy of both simulations. When compared with ALF, it has shown good accuracy, computational efficiency, and convergence properties.

Key-Words: - ALF, Complex power system, IEEE 57 bus, MATPOWER, PF, Scaled Load, SLF, Steady-Stat.

Received: March 12, 2023. Revised: December 4, 2023. Accepted: December 24, 2023. Published: December 31, 2023.

1 Introduction

MATPOWER is an open-source MATLAB power system tool that is mostly used in academic research for AC and DC power flow (PF) and optimal power flow (OPF). It consists of a predetermined set of m-files, which are designed to give the best performance of simulation, [1], for any problem formulation. It has become a more popular tool today for high-level computation languages. Therefore, it is very suitable to study steady-state power systems. When comparing the use of MATPOWER with earlier days, it is growing day by day, with about 50% for academia, 43% for research, and 7% for industry and others, [2]. The main motivation for the development of this tool is to design a MATLAB-based PF and OPF to achieve the computational requirements of the Power Web platform, which is a web-based testing simulation platform used in the electricity markets, [3], [4]. It requires software that uses the OPF for the computation of power allocation and the pricing of electrical energy. Due to its clear potential and usefulness to the researchers, MATPOWER was released as open-source software through the Internet. The extensive OPF architecture in this problem has allowed the researchers to add new variables, constraints, and costs to the standard problem, [5]. For the operation and planning purposes of a power system network, a stochastic method was proposed that can maximize the total expected benefits for planning, incorporation of costs, and benefits of electricity consumption, power generation, services, storage, and load shedding. However, the uncertainty was modelling for maintenance of the power system security and for proper representation of stochastic cost, [6]. Deregulation markets in power systems always look for robust OPF, whereas they should provide deterministic convergence, accurate computation of prices, smooth costing, etc. Instead of the advancements that have been made, [7], [8], [9], [10], [11], [12], the ACOPF was not adopted in the real-time operation of complex power systems. In the reference, [13], three new OPF methods were proposed: the Trust Region-Based Augmented Lagrangian Method (TRALM), the Step-Controlled primal-dual Interior Point Method (SCIPM), and the Constrained Cost Variable (CCV) formulations. The MOST, [14] is used to compare and analyze the stochastic day-ahead Security Constrained Unit Commitment (SUCC) in the traditional approach. In the reference, [15], it is shown that this tool is used to compare multi-stage uncertainties and reduce the effect of modelling assumptions on the power system.

MATPOWER is facilitated by an extensive suite of tests to ensure the quality of the code. Many researchers are using this to find the testing framework for designing their own MATLAB programs. There are various software packages used for power system simulation developed by the researchers. MATLAB / Simulink has been supported in designing the power system which includes power electronics, FACTS, control systems, renewable sources, etc. The state-space modelling and GUI-based PSB components are discussed in, [16]. Simulink has been developed as an educational package since 1997. ULg was collaborated with Bologna University and developed various traditional components such as synchronous generators, transmission lines, transformers, etc. in the Electrical Energy Systems Lab. of NTUA, [17]. A Power Analysis Toolbox (PAT) was developed by the West Virginia Universities Advanced Power Engineering Research Centre (APERC), it includes FACTS, flexible to perform load flow, transient, and small signal analysis of power systems, [18]. Mat Dyn is open-source software meant to focus on transient stability analysis and time domain simulation. The design criteria, advantages, and code structure are discussed in, [19]. The PSAT was the first open-source software that was runs on the GNU / Octave and network editor to perform power system analysis. Other than those features, it has continuation power flow (CPF), GUI, and GNE, [20]. It has been used by many universities for teaching both UG and PG courses and also formed an online virtual laboratory to support the students via Internet, [21], [22].

Analysis of a bulk power system network is a very tedious task due to the greater number of interconnections between the transmission lines and the many components connected to it. Each component has its own characteristics and posture and is meant for a particular goal. Therefore, it is very difficult to understand the interactions in a network and the representation of its behavior with mathematical equations, [23], [24]. The dynamic behavior of such a system is more important, so it is very essential to increase stability when the electrical loads in the system are increasing. In addition to that, it is very essential to study the changes in generation, load, and disturbances. Therefore, it is required to monitor the operating conditions by using a real-time power system model that should be useful for power system operators to analyze the power system model during abnormal threats, [25], [26]. The design of such a high-voltage power system network is practically impossible because of the constraints involved in its huge dimensions, high rating of equipment, and complex system theory. Therefore, it is essential to design such complex power system networks in the laboratory for analysis, and that network should possess characteristics that are similar to the original network, [27]. Generally, the power system consists of various components that would be deployed for electrical supply, power transfer, and use of supply. In the power system network, the synchronous generators would supply electrical power, and transmission lines would carry power to loads such as homes, industries, etc. The analysis of a multi-machine power system network consisted of the study of power transfer in transmission lines, [28], continuous monitoring of control, supervision, and protection under steady-state operation and contingency conditions. In addition to those, it is very essential to capture the behavior of the network within a time span of a few microseconds to several hours, or even for years. This was found by using static, dynamic, and transient analyses. However, it is found that the type of study and its objectives are changing from one power system to another, even though they would have identical prospective and the same analysis modules, [29].

The modelling of a practical power system network is a critical task in terms of successful operation and management. The MATPOWER tool is very useful to test the power system in an off-line environment so that it would verify the operation of network to plan and optimize in a correct way to model the power system. The main aim of this paper is to design a scaled-load steady-state model of the IEEE 57 bus power system network, [30]. The proposed system consists of 57 buses, 42 PQ loads, 7 PV generators, 63 positive sequence pi model transmission lines, and 17 transformers. The scale load (SL) procedure is used to derive the ratings of loads and generators by using the specific SL ratio of each bus. According to the standard system data, it has 138kv (from 1 to 17 buses) and 69kv (from 18 to57 buses, the SL derived for each bus by using the voltages 414 volts and 207 volts respectively. The standard Newton-Raphson (NR) AC power flow method is used for finding the bus voltage, phase angle, and power flow in lines. As per the standard test case data modification of loads and generators made in the MATPOWER extensible case 57 structures for ALF and SLF simulations, The simulation results have shown the accuracy, efficiency, and computation of the SL procedure used in this paper. It also, helps to understand the behavior of a power system network when it is mathematically well-conditioned at low voltages. The evaluation of results is useful to design a hands-on equivalent circuit practically. It can be used for various power system experimentations in academic research.

The fore coming sections are explained as follows, the Section 2 discussed about the Scaled Power Flow procedure and modifications of loads in case structure. The IEEE 57 bus power system model summary is explained in Section 3. The comparison of voltage, phase angle, and power flow results is explained in Section 4. Accuracy of results and conclusions are discussed in Section 5.

2 Scaled Load Flow Formulation

The traditional power flow problem is used to find voltage, phase angle, and power flows in lines for specified load and generation patterns. Normally, in MATPOWER, the power flow is executed by calling runpf with a case structure. Whether it is AC or DC power flows, the solution to the set of equations is in the form of:

$$g(x) = 0 \tag{1}$$

The above equation is defined to derive the subset of the bus power balance equation in the polar coordinate's method as a function of unknown voltages. The AC power balance equation is obtained from the matched bus injections of the loads and generators. It is expressed as a function of the bus voltage and generator injections in complex matrix form.

$$gS(V, S_g) = S_{bus}(V) + S_d - C_g S_g = 0 \tag{2}$$

2.1 A.C Power Flow

In AC power flow, by convention, one of the generators is considered a slack bus; it serves as a voltage reference and real power. Although the real power at this bus is specified as unknown to avoid overstating the problem, the remaining generator buses are considered PV buses; these buses are specified with voltage and real power injection. Remaining all the buses are considered as load buses (i.e., PQ) with specified active and reactive power load demands. The power balance in power flow is expressed in polar coordinates as a function of voltage, phase angle, generator injections, and constant load demands.

$$gP\left(\Theta, V_m, P_g\right) = P_{bus}(\Theta, V_m) + P_d - C_g P_g = 0 \tag{3}$$

$$gQ(\Theta, V_m, Q_g) = Q_{bus}(\Theta, V_m) + Q_d - C_g Q_g = 0 \tag{4}$$

For $g(x)$ function, let us consider the equations (3) & (4) for all buses except slack bus. Where, I_{ref}, I_{PV}, and I_{PQ} are the refernce bus, PV bus, and PQ bus respectively. Therefore,

$$g(x) = \begin{pmatrix} g_P^i(\Theta, V_m, P_g) & \forall i \in I_{PV} \cup I_{PQ} \\ g_Q^i(\Theta, V_m, Q_g) & \forall j \in I_{PQ} \end{pmatrix} \tag{5}$$

Where the x consists of voltages of PQ buses and phase angles of non-reference buses. It is derived as,

$$g(x) \tag{6}$$

The Eq. 6 derives $n_{PV} + 2n_{PQ}$ non-linear equations and unknown values, where n_{PV} and n_{PQ} are number of PV and PQ buses respectively. After the solution of Eq. 5 the Eq. 3 compute the slack bus real power injection. In addition to that the $n_{PV} + 1$ equations derive the PV buses reactive power injections.

2.2 Scaled Power Flow

MATPOWER has pre-defined extensible structures; it can allow modifications and additions to the standard problem. In the research point of view, this tool is very desirable for modifying the problem without overwriting the standard power flow problem, [2], [3], [4], [5], according to the requirements. In this paper, Scaled-Load (SL) function is used to scale active and reactive powers in the network according to the base voltage specified in, [30], for the design and verification of the power flow of a low-voltage power system network. In this paper, the authors designed a low-voltage IEEE 57 bus model. Let us consider that the physical properties of the load and generator are constant. Therefore, the SL is the ratio of the actual bus voltage to the scaled voltage of the ith bus.

$$SL = \frac{V_{act}^i}{V_{sc}^i} \tag{7}$$

The quantity of scaling of active power and reactive power are based on the SL which are derived by the Eq. 7. Whereas the active power is directly proportional to the square of the voltage ($P \propto V^2$), therefore the scaled active power of i^{th} the bus is as follows:

$$P_{sc}^{i} = \frac{P_{act}^{i}}{SL^2} \tag{8}$$

Similarly, the reactive power also directly proportional to the square of the voltage ($Q \propto V^2$), therefore the scaled reactive power of the i^{th} bus also as,

$$Q_{sc}^{i} = \frac{Q_{act}^{i}}{SL^2} \tag{9}$$

The Eq. 8 and Eq. 9 are used to specify the ratings of loads and generators in the scaled power system. Therefore, based on the direct scaling factor SL the scaled load and generator rating are specified with in the IEEE 57 bus base case structure for Scaled Load Flow (SLF) model for analysis with the Actual Load Flow (ALF).

3 Power System Modeling

The present work aims to design a Scaled load flow (SLF) model of an IEEE 57 bus power system network. Referring to the single-line diagram of the network shown in Figure 1, it consists of information about the interconnection of transmission lines to the buses, generators, loads, and location of transformers, as well as all the components' standard data, like voltage and power, considered from standard system data. The power system has 57 buses; among those, up to 17 buses are specified with a voltage of 138 kV, and reaming buses are specified with a voltage of 69 kV. For the design of the scaled load model, these voltages are scaled to 414 volts and 207 volts, respectively.

The load flow analysis for this work uses standard steady-state models. The NR load flow analysis uses the following AC simplified models, which are referenced in, [1], [2].

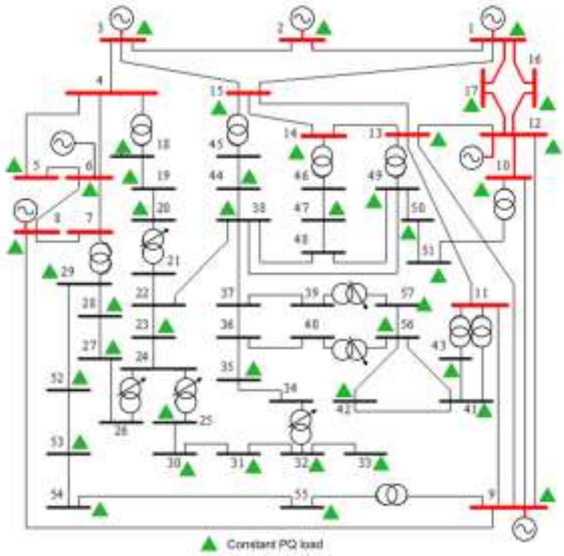

Fig. 1: IEEE 57 Bus Power System network single-line block diagram.

4 Result Analysis

This section has discussed the simulations of both ALF and SLF case models, whereas the ALF is modelled according to the standard IEEE 57 bus case data. The SLF is modelled by editing the case structure fields such as base MVA, bus load data, and generator data as per the scaled values; however, the bus voltages are already expressed in the p.u. values. The polar coordinate load flow solution is obtained by using power balance Eq. 2, and the AC NR load flow simulation converged in 3 iterations for both models. The similarity between the ALF and SLF models has been compared with the MATPOWER function of compare_case. It has verified the bus, branch, and generator matrixes of two models of each column and printed any non-zero differences.

4.1 Load Flow Analysis of Actual and Actual and Scaled Power Systems

Table 1 (Appendix) shows the bus voltage results of both load flows. The ALF has converged in 1.61 seconds. The total active power generation of the system is 1975.9 Mw, and the reactive power is limited to 699 Mvar. The minimum voltage is found at 0.936 p.u. at bus 31, and the maximum voltage is found at 1.06 p.u. at bus 46. The magnitude of the maximum phase angle is 19.51 deg, which is at bus 31. Similarly, when the results of SLF are observed, they converge in 0.19 seconds. The total active power generation capacity of this system is 17.78 kw, and the maximum reactive power is limited to 4.5 kvar. The minimum voltage is found on the same 31 bus as in ALf, but the magnitude is 0.904 p.u.; likewise, the maximum voltage is also on bus 46, but the magnitude is 1.057 p.u. The maximum phase is like in ALF on the same bus. However, the minimum phase angle is zero deg, which is found on bus 1 in both simulations.

The power system consists of 42 fixed PQ loads. As shown in Table 2 (Appendix), the line flows are similar in both simulations of the system. The actual system has 1250.8 Mw of active power and 321.1 Mvar of reactive power. The simulation results have shown that the total line active power loss is 27.86 Mw and 121.67 Mvar of reactive power losses. However, the maximum active power loss is 3.9 Mw and the reactive power loss is 19.96 Mvar, as found in lines 1–15. Similarly, when a scaled power system is considered, it has 11.26 kw of active power and 3.02 kvar of reactive power loads. The simulation result of the scaled system has shown that the total active power loss is 255.5 watts and the reactive power loss is 1.11 kvar. Although the losses found in lines 1–15 are the same as in ALF, the maximum active power loss is 35.31 watts and the maximum reactive power is 180.5 var.

4.2 Comparative Analysis

This section has shown the comparative analysis of voltage, phase angle, line power flows, and percentage of losses of line powers from Figure 2 to Figure 7. This analysis is very useful to compare the results on any bus and in any line. Figure 2 shows that the bus voltage has decreased at most of the buses for the SLF solution.

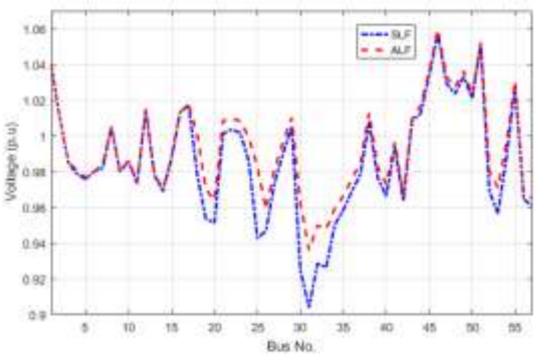

Fig. 2: Magnitude of bus voltage in p.u.

When comparing phase angles in Figure 3, there is no difference between phase angles. However, negligible differences were found at buses 31, 32, and 33.

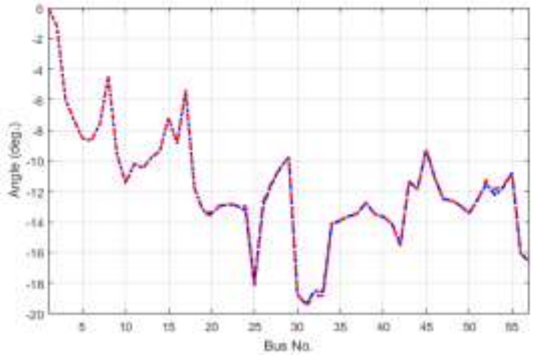

Fig. 3: Magnitude of phase angle at bus in deg.

As shown in Figure 4, the active power flow in the transmission lines from the bus is the same in all. However, few lines have carried more active power; those lines are 1-2, 2-3, 8-9, 1-15, 1-16, and 1-17, most of them connected to bus 1.

Similarly, Figure 5 shows the reactive power of transmission lines in the view of the bus, which is the same for all lines. However, lines 1-2 and 12–13 have carried more reactive power.

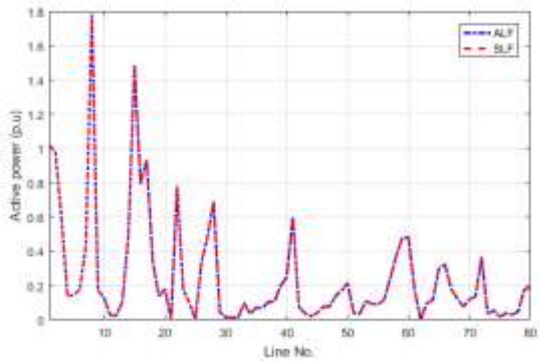

Fig. 4: From bus active power of transmission line.

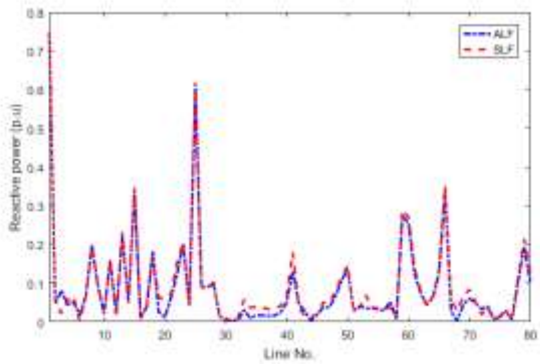

Fig. 5: From bus reactive power of transmission line.

Figure 6 and Figure 7 show the percentage of active and reactive power losses, respectively. Maximum power losses are found in lines 1-2, 2-3, 8-9, 1-15, 1-6, and 1-17. As shown in Figure 6, all the transformers carry zero active power; the maximum power loss is found at 3.9% in lines 1–15. Even though there is no active power loss in the transformer, the reactive power has flown in all; the maximum reactive power is 19.96%, which is found in the same line.

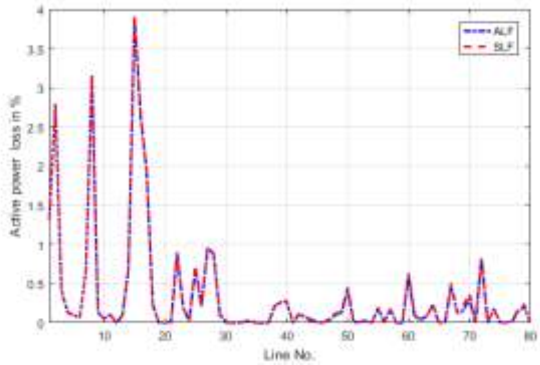

Fig. 6: Transmission line active power loss in percentage.

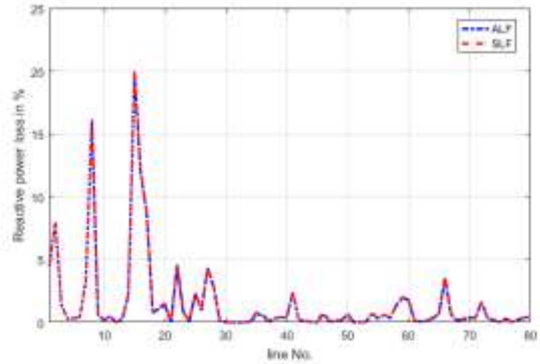

Fig. 7: Transmission line reactive power loss in percentage.

5 Conclusions

In this work, the scaling procedure was used to design a low-voltage power flow model of an IEEE 57 bus power system network. The scaled model was designed by using the actual SL factor, which is derived from the actual system voltages and scaling voltages. By using the power balance method, the NR load flow solution is obtained for both the ALF and SLF models. The simulation results have been thoroughly compared for analysis of the accuracy of the scaling method, and it was shown that the suggested scaling procedure can be used to design practical low-voltage power system models. The analysis of the results has shown good computational capacity, efficiency, accuracy, and robust behaviour-scaling procedures. A better understanding of this scaled modelling procedure is very useful for designing the low-voltage real-time power system model. It is very useful in academic research to assess the real-time performance of power systems. The results presented in this paper are very useful for designing a low-voltage IEEE 57 bus-equivalent network model. This model can help researchers assess the real-time behaviour of the network for various power system research applications.

Acknowledgment:
We would like to show our gratitude to Vignan's Foundation for Science, Technology, and Research for their encouragement during this work.

References:

[1] Magrini, Ray D Zimmerman and Carlos E Murillo-S´anchez. Matpower 6.0 user’s manual. *Power Systems Engineering Research Center*, 2016.

[2] Zimmerman, R. D., Murillo-Sánchez, C. E., & Thomas, R. J. (2010). MATPOWER: Steady-state operations, planning, and analysis tools for power systems research and education. *IEEE Transactions on power systems*, 26(1), 12-19.

[3] Katuri, R., & Gorantla, S. (2020). Modeling and analysis of hybrid controller by combining MFB with FLC implemented to ultracapacitor-based electric vehicle. *WSEAS Transactions on Power Systems*, 15, 21-29.

[4] Teh, J., & Lai, C. M. (2019). Reliability impacts of the dynamic thermal rating system on smart grids considering wireless communications. *IEEE Access*, 7, 41625-41635.

[5] Cheng, Q., Lin, X., Peng, S., Tang, J., Ponci, F., & Monti, A. (2022). Efficient and Robust Power Flow Algorithm for Asynchronous Grids Coupled Through a VSC-MTDC System and Its Probability Analysis. *IEEE Systems Journal*, 17(2), 3270-3281.

[6] Murillo-Sánchez, C. E., Zimmerman, R. D., Anderson, C. L., & Thomas, R. J. (2013). Secure planning and operations of systems with stochastic sources, energy storage, and active demand. *IEEE Transactions on Smart Grid*, 4(4), 2220-2229.

[7] Triwijaya, S., Sugiantoro, N., Prasetyo, Y., Wibowo, R. S., & Penangsang, O. (2018). Security constrained optimal power flow considering dynamic line rating. *In 2018 10th International Conference on Information*

Technology and Electrical Engineering (ICITEE) (pp. 46-51). IEEE.

[8] Yao, M., Molzahn, D. K., & Mathieu, J. L. (2019). An optimal power-flow approach to improve power system voltage stability using demand response. *IEEE Transactions on Control of Network Systems*, 6(3), 1015-1025.

[9] Martins, R., Kreimer, P., & Musilek, P. (2017). LP-based predictive energy management system for residential PV/BESS. *In 2017 IEEE International Conference on Systems, Man, and Cybernetics (SMC)* (pp. 3727-3732). IEEE.

[10] Li, S., Wang, D., Zhu, Y., Liu, L., & Jia, H. (2020). Multi-objective optimal control based on practical security region of regional integrated energy system. *In 2020 IEEE Power & Energy Society General Meeting (PESGM)* (pp. 1-5). IEEE.

[11] Li, Z., Yu, J., & Wu, Q. H. (2017). Approximate linear power flow using logarithmic transform of voltage magnitudes with reactive power and transmission loss consideration. IEEE Transactions on Power Systems, 33(4), 4593-4603.

[12] Chen, P., Sun, K., Zhang, C., & Sun, B. (2021). A Feasible Zone Analysis Method with Global Partial Load Scanning for Solving Power Flow Coupling Models of CCHP Systems. Journal of Modern *Power Systems and Clean Energy*, 10(2), 371-377.

[13] Campanhol, L. B. G., Da Silva, S. A. O., De Oliveira, A. A., & Bacon, V. D. (2018). Power flow and stability analyses of a multifunctional distributed generation system integrating a photovoltaic system with unified power quality conditioner. *IEEE Transactions on Power Electronics*, 34(7), 6241-6256.

[14] Lamadrid, A. J., Munoz-Alvarez, D., Murillo-Sánchez, C. E., Zimmerman, R. D., Shin, H., & Thomas, R. J. (2018). Using the Matpower Optimal Scheduling Tool to Test Power System Operation Methodologies under Uncertainty. *IEEE Transactions on Sustainable Energy*, 10(3), 1280-1289.

[15] Henriques, R. M., Passos Filho, J. A., & Taranto, G. N. (2021). Determining Voltage Control Areas in Large Scale Power Systems Based on Eigenanalysis of the QV Sensitivity Matrix. *IEEE Latin America Transactions*, 19(02), 182-190.

[16] Li, C., Wu, Y., Zhang, H., Ye, H., Liu, Y., & Liu, Y. (2020). STEPS: a portable dynamic simulation toolkit for electrical power system studies. *IEEE Transactions on Power Systems*, 36(4), 3216-3226.

[17] Sun, D., Liu, H., Gong, M., Chen, Z., & Hart, P. (2023). A stability analysis tool for bulk power systems using black-box models of inverter-based resources. *IEEE Transactions on Industry Applications*, 59(6), 7318-7327.

[18] Kucuk, I., Thangamani, T., Murkowska, M. I., Souvirta, M., Satheesh, S., Højgaard, F. N., & Bak, C. L. (2020). Managing harmonics in wind power plants using the control of wind turbines. *In 2020 IEEE Power & Energy Society General Meeting (PESGM*) (pp. 1-5). IEEE.

[19] Wu, H., Qiu, Y., He, Z., Dong, S., & Song, Y. (2019). A Free and Open Source Toolbox based on Mathematica for Power System Analysis. *In 2019 IEEE Power & Energy Society General Meeting (PESGM)* (pp. 1-5). IEEE.

[20] Phongtrakul, T., Kongjeen, Y., & Bhumkittipich, K. (2018). Analysis of power load flow for power distribution system based on pypsa toolbox. *In 2018 15th International Conference on Electrical Engineering/Electronics, Computer, Telecommunications and Information Technology (ECTI-CON)*, pp.764-767, IEEE.

[21] Katuri, R., & Gorantla, S. (2020). Realization of prototype hardware model with a novel control technique used in electric vehicle application. *Electrical Engineering*, 102(4), 2539-2551.

[22] Vanfretti, L., & Milano, F. (2011). Facilitating constructive alignment in power systems engineering education using free and open-source software. *IEEE Transactions on Education*, 55(3), 309-318.

[23] Thurner, L., Scheidler, A., Schäfer, F., Menke, J. H., Dollichon, J., Meier, F., & Braun, M. (2018). pandapower—an open-source python tool for convenient modeling, analysis, and optimization of electric power systems. *IEEE Transactions on Power Systems*, 33(6), 6510-6521.

[24] Dong, X., Sun, H., Wang, C., Yun, Z., Wang, Y., Zhao, P., & Wang, Y. (2017). Power flow analysis considering automatic generation control for multi-area interconnection power networks. *IEEE Transactions on Industry Applications*, 53(6), 5200-5208.

[25] Katuri, R., & Gorantla, S. (2020). Optimal performance of Lithium-Ion battery and ultra-capacitor with a novel control technique used

in e-vehicles. Journal of New Materials for Electrochemical Systems, 23(2), 139-150.

[26] Chen, R. L. Y., Cohn, A., Fan, N., & Pinar, A. (2014). Contingency-risk informed power system design. *IEEE Transactions on Power Systems*, 29(5), 2087-2096.

[27] Cataliotti, A., Cosentino, V., Di Cara, D., Russotto, P., Telaretti, E., & Tinè, G. (2015). An innovative measurement approach for load flow analysis in MV smart grids. *IEEE Transactions on Smart Grid*, 7(2), 889-896.

[28] Zhao, Y., Goldsmith, A., & Poor, H. V. (2016). Minimum sparsity of unobservable power network attacks. *IEEE Transactions on Automatic Control*, 62(7), 3354-3368.

[29] Abdi-Khorsand, M., & Vittal, V. (2016). Modeling protection systems in time-domain simulations: A new method to detect mis-operating relays for unstable power swings. *IEEE Transactions on Power Systems*, 32(4), 2790-2798.

[30] Rossoni, P., da Rosa, W. M., & Belati, E. A. (2016). Linearized AC load flow applied to analysis in electric power systems. *IEEE Latin America Transactions*, 14(9), 4048-4053.

APPENDIX

Table 1. Bus voltage results of both actual and scaled Load Flows

bus	RLF		ALF	
	V (volts)	Angle (deg.)	V (volts)	Angle (deg.)
1	1.040	0.000	1.040	0.000
2	1.010	-1.189	1.010	-1.188
3	0.985	-5.992	0.985	-5.988
4	0.979	-7.297	0.981	-7.337
5	0.976	-8.543	0.976	-8.546
6	0.980	-8.687	0.980	-8.674
7	0.982	-7.589	0.984	-7.601
8	1.005	-4.496	1.005	-4.478
9	0.980	-9.613	0.980	-9.585
10	0.986	-11.484	0.986	-11.450
11	0.973	-10.213	0.974	-10.193
12	1.015	-10.497	1.015	-10.471
13	0.978	-9.818	0.979	-9.804
14	0.969	-9.358	0.970	-9.350
15	0.987	-7.194	0.988	-7.190
16	1.013	-8.877	1.013	-8.859
17	1.017	-5.406	1.017	-5.396
18	0.978	-11.748	1.001	-11.730
19	0.953	-13.345	0.970	-13.227
20	0.951	-13.591	0.964	-13.444
21	1.001	-12.887	1.008	-12.929
22	1.004	-12.837	1.010	-12.874
23	1.002	-12.888	1.008	-12.940
24	0.986	-12.988	0.999	-13.292
25	0.943	-18.022	0.983	-18.173
26	0.947	-12.678	0.959	-12.981
27	0.974	-11.399	0.982	-11.514
28	0.990	-10.431	0.997	-10.482
29	1.005	-9.764	1.010	-9.772
30	0.925	-18.667	0.963	-18.720
31	0.904	-19.512	0.936	-19.384
32	0.929	-18.792	0.950	-18.512
33	0.926	-18.833	0.948	-18.552
34	0.950	-14.089	0.959	-14.149
35	0.958	-13.867	0.966	-13.906
36	0.969	-13.614	0.976	-13.635
37	0.979	-13.432	0.985	-13.446
38	1.008	-12.726	1.013	-12.735
39	0.977	-13.480	0.983	-13.491

bus	RLF		ALF	
	V	Angle	V	Angle
	(volts)	(deg.)	(volts)	(deg.)
40	0.966	-13.643	0.973	-13.658
41	0.994	-14.118	0.996	-14.077
42	0.964	-15.556	0.967	-15.533
43	1.008	-11.379	1.010	-11.354
44	1.013	-11.857	1.017	-11.856
45	1.034	-9.291	1.036	-9.270
46	1.057	-11.141	1.060	-11.116
47	1.030	-12.537	1.033	-12.512
48	1.023	-12.626	1.027	-12.611
49	1.033	-12.971	1.036	-12.936
50	1.021	-13.454	1.023	-13.413
51	1.051	-12.578	1.052	-12.533
52	0.969	-11.249	0.980	-11.498
53	0.956	-11.874	0.971	-12.253
54	0.988	-11.560	0.996	-11.710
55	1.028	-10.847	1.031	-10.801
56	0.965	-16.064	0.968	-16.065
57	0.961	-16.576	0.965	-16.584

Table 2. From bus active and reactive powers of both Actual and scaled load flows

FB	TB	Scaled load flow		Actual load flow	
		Pf	Qf	Pf	Qf
		(watts)	(var)	(Mwatts)	(Mvar)
1	2	919.32	674.83	102.09	75.00
2	3	880.47	-41.89	97.77	-4.64
3	4	538.90	-19.88	60.21	-8.18
4	5	123.50	-49.31	13.80	-4.43
4	6	128.65	-59.10	14.16	-5.09
6	7	-159.97	2.70	-17.78	-1.71
6	8	-382.14	-59.18	-42.50	-6.56
8	9	1605.48	178.10	178.03	19.83
9	10	155.43	-80.85	17.17	-9.23
9	11	116.47	25.31	12.90	2.07
9	12	22.81	-142.66	2.55	-15.85
9	13	20.89	-12.95	2.32	-1.96
13	14	-92.45	209.12	-10.35	22.34
13	15	-441.01	44.09	-48.89	4.89
1	15	1342.11	312.16	148.99	33.79
1	16	714.68	-7.84	79.25	-0.87
1	17	841.54	35.41	93.34	3.94
3	15	307.41	-151.30	33.77	-18.19
4	18	124.13	55.53	13.96	2.44

FB	TB	Scaled load flow		Actual load flow	
		Pf (watts)	Qf (var)	Pf (Mwatts)	Qf (Mvar)
4	18	158.90	53.80	17.87	1.19
5	6	5.28	-65.69	0.67	-6.24
7	8	-698.51	-137.96	-77.94	-12.41
10	12	-159.97	-183.50	-17.60	-20.09
11	13	-89.54	-37.14	-9.93	-4.39
12	13	-3.39	556.18	-0.49	60.35
12	16	-301.92	79.91	-33.40	8.82
12	17	-437.50	83.03	-48.46	9.17
14	15	-621.36	-92.64	-68.84	-9.60
18	19	38.23	6.05	4.63	1.39
19	20	7.72	-0.54	1.23	0.63
21	20	13.00	9.82	1.08	0.39
21	22	-13.00	-9.82	-1.08	-0.39
22	23	86.81	52.13	9.65	3.11
23	24	30.00	33.06	3.34	1.00
24	25	62.08	35.16	7.07	1.71
24	25	59.65	33.79	6.79	1.65
24	26	-92.14	-29.07	-10.54	-1.55
26	27	-92.14	-29.62	-10.54	-1.61
27	28	-177.76	-37.06	-20.04	-2.43
28	29	-221.55	-61.45	-24.90	-5.13
7	29	537.94	161.52	60.09	13.03
25	30	65.03	31.91	7.56	4.63
30	31	31.75	14.38	3.85	2.66
31	32	-20.97	-12.50	-2.03	-0.35
32	33	34.27	17.17	3.81	1.91
34	32	70.05	45.24	7.46	3.79
34	35	-70.05	-45.24	-7.46	-3.79
35	36	-124.49	-70.27	-13.50	-6.55
36	37	-156.58	-104.36	-17.07	-10.61
37	38	-192.18	-130.73	-21.05	-13.70
37	39	34.39	24.83	3.86	2.93
36	40	31.03	34.11	3.46	4.09
22	38	-99.83	-61.99	-10.73	-3.51
11	41	82.91	33.60	9.19	3.53
41	42	79.91	31.41	8.88	3.27
41	43	-104.66	-28.83	-11.59	-2.95
38	44	-220.68	34.44	-24.35	5.23
15	45	337.66	6.43	37.33	-0.73
14	46	433.57	260.70	47.89	27.40
46	47	433.57	242.67	47.89	25.47
47	48	160.61	124.67	17.59	12.43

FB	TB	Scaled load flow		Actual load flow	
		Pf (watts)	Qf (var)	Pf (Mwatts)	Qf (Mvar)
48	49	-0.40	-71.56	0.08	-7.38
49	50	84.66	35.37	9.66	4.43
50	51	-105.04	-60.25	-11.42	-6.20
10	51	269.21	117.47	29.64	12.51
13	49	292.61	315.12	32.43	33.80
29	52	160.89	51.14	17.92	2.55
52	53	112.27	25.47	12.55	-0.25
53	54	-68.93	-60.31	-7.57	-4.47
54	55	-107.74	-75.27	-11.82	-6.06
11	43	122.66	46.11	13.59	4.85
44	45	-330.26	16.88	-36.52	3.28
40	56	30.95	33.99	3.46	4.07
56	41	-49.34	4.00	-5.43	0.66
56	42	-14.21	11.25	-1.58	1.46
39	57	34.34	24.75	3.85	2.92
57	56	-25.96	4.04	-2.85	0.61
38	49	-43.58	-103.17	-4.66	-10.53
38	48	-158.11	-191.96	-17.22	-19.39
9	55	172.35	115.63	18.93	10.38

Contribution of Individual Authors to the Creation of a Scientific Article (Ghostwriting Policy)

The authors equally contributed in the present research, at all stages from the formulation of the problem to the final findings and solution.

Sources of Funding for Research Presented in a Scientific Article or Scientific Article Itself

We would like to show our gratitude to Vignan's Foundation for Science, Technology, and Research for their encouragement during this work.

Conflict of Interest

The authors have no conflicts of interest to declare.